Pergamon

Int. J. Solids Structures Vol. 35, Nos 31–32, pp. 4295–4311, 1998

0020–7683/98 $19.00 + .00

PII: S0020–7683(97)00317–X

COUPLINGS IN EARLY-AGE CONCRETE: FROM MATERIAL MODELING TO STRUCTURAL DESIGN

FRANZ-JOSEF ULM*
Laboratoire Central des Ponts et Chaussées, Div. Bétons and Ciments pour Ouvrages d'Art; 58, Bd. Lefebvre; 75732 Paris Cedex 15, France

and

OLIVIER COUSSY
Laboratoire Central des Ponts et Chaussées, Service Modélisation pour l'Ingénieur; 58, Bd. Lefebvre; 75732 Paris Cedex 15, France

(*Received* 21 *October* 1996; *in revised form* 31 *July* 1997)

Abstract—Couplings in early-age concrete are the cross-effects between the hydration reaction, temperature evolution and deformation which can lead to cracking. They involve complex chemo-physical mechanism that operate over a broad range of scales, from nanometer to meter. This paper explores these thermo-chemo-mechanical cross-effects from the macroscale of engineering material modeling (the typical scale of laboratory test specimens) to the level of structural design. Set within the framework of chemoplasticity, the cross-effects in the constitutive model are derived from Maxwell-symmetries, and characterize the autogeneous shrinkage, hydrate heat and strength growth due to the chemo-mechanical, thermo-chemical and chemo-plastic couplings. These couplings at a material level can be determined from standard material tests, provided that the order of coupling is known. This is shown by considering adiabatic calorimetric experiments and isothermal strength growth tests, which lead to identify an intrinsic kinetics function that characterizes the macroscopic hydration kinetics of concrete. Finally, an example of application of the model to large-scale finite element analysis of concrete structures is presented, which clearly shows the consequences of thermo-chemo-mechanical couplings for the engineering design of concrete structures at early ages.

1. INTRODUCTION

Couplings in early-age concrete are the cross-effects between the hydration reaction, temperature evolution and deformation which can lead to cracking. They involve complex chemo-physical mechanisms that operate over a broad range of scales, from nanometer to meter. Their account in the design of civil engineering structures is generally based upon semi-empirical approaches which, as far as the material is concerned, mainly consist in extrapolating laboratory test results to the field conditions occurring in the structure. This extrapolation is for its major part achieved through mathematical models fitting the experimental observations. In order to reproduce adequately the various field conditions and to simulate the corresponding material response, a great number of test results is required. To reduce the number of tests, the intrinsic behavior related to the hydration reaction and its coupling with temperature evolution and deformation needs to be extracted from the observations, and integrated in the constitutive modeling of early-age concrete. This approach is necessarily based upon a qualitative understanding of the underlying micro-processes of the hydration reaction, and its links with the macroscopic observable material behavior. For instance, the link between the mechanical compressive strength and the hydration degree has been a matter of research for quite some time: Mindess *et al.* (1978) showed that the compressive strength increases quasi-linearly with the hydration products. The same has been found for concrete by Byfors (1980), and Regourd and Gauthier (1980) studied the kinetics of the compressive strength evolution and related it to that of the hydration reaction. Similar experimental relations have been established for the

* Author to whom correspondence should be addressed. E-mail: ulm@lcpc.fr.

elastic properties of the hydrating concrete (e.g. Laube, 1990; Torrenti, 1992; Boumiz *et al.*, 1996).

This paper revisits these experimental established cross-effects from the standpoint of constitutive modeling of thermo-chemo-mechanical couplings in early-age concrete that aims at predicting the deformation and cracking at the macroscopic level of material description. Set within the framework of reactive porous media (cf Coussy, 1995), the modeling of thermo-chemo-mechanical couplings of concrete at early ages has been presented in Ulm and Coussy (1995), and extended to irreversible skeleton evolution on account of strength-growth as chemo-plastic hardening recently (Ulm and Coussy, 1996). This paper is concerned with identification, experimental determination and consequences for structural design of thermo-chemo-mechanical couplings in early-age concrete.

2. CONSTITUTIVE MODELING OF THERMO-CHEMO-MECHANICAL COUPLINGS

In this part, some basic relations on thermo-chemo-mechanical couplings of concrete at early ages are briefly recalled. As shown hereafter, by using the thermodynamic framework of chemically reactive porous media, these coupling terms result from Maxwell-symmetries.

Consider cement paste or concrete as a porous medium composed of a skeleton and some fluid phases saturating the macro-porous space (capillary pores the width of which are larger than 1 μm). For the sake of clarity the elementary system is considered as closed with respect to the fluid phases saturating the porous space (i.e. water, vapor and dry air in the macropores of cementious materials). The solid part of the matter is formed of unhydrated cement and hydrates. The observable strain is that of the skeleton and is noted $\boldsymbol{\varepsilon}$. We note $\boldsymbol{\varepsilon}^p$ and χ, respectively, the plastic (or permanent) strain tensor and some hardening/softening variables, which represent in the macroscopic modeling the irreversible skeleton deformation (for instance micro-cracking). Furthermore, in order for the hydration reaction to occur, water diffuses to the unhydrated cement through the layers of hydrates already formed. Once they meet, new hydrates are formed in a quasi instantaneous manner, relative to the time scale of the micro-diffusion process, and the water is then chemically and/or physically combined. We note m the hydrate mass per unit of volume, which equals with opposite sign the variation of the liquid water phase per unit of macroscopic volume (mass-conservation in the closed porous medium).

Applying standard thermodynamics, the intrinsic dissipation of the closed system reads:

$$\varphi = \boldsymbol{\sigma} : \dot{\boldsymbol{\varepsilon}} - S\dot{T} - \Psi \geqslant 0 \tag{1}$$

where a dot denotes time derivative, $\boldsymbol{\sigma}$ = macroscopic stress tensor related by mechanical equilibrium to the external forces, S = entropy, T = (absolute) temperature, and Ψ = Helmholtz free energy introduced here as volume density. The latter reads as a function of the state variables which characterize the energy state of the elementary system. These are here strain $\boldsymbol{\varepsilon}$ and temperature T as external state variables, and the internal state variables $\boldsymbol{\varepsilon}^p$ and χ. Furthermore, in the case of closed reactive porous media, also the variation of hydrate mass m is part of the set of internal state variables (i.e. not controlled from the exterior, for a detailed derivation from mass-conservation and thermodynamics of open porous continua, see Coussy, 1995). Free energy Ψ is assumed formally:

$$\Psi = \Psi(T, \boldsymbol{\varepsilon}, \boldsymbol{\varepsilon}^p, \chi, m) = \psi(\boldsymbol{\varepsilon} - \boldsymbol{\varepsilon}^p, T, m) + U(\chi, m) \tag{2}$$

where $U(\chi, m)$ is the part of free energy associated with plastic hardening/softening phenomena in the material, as detailed later on. Then, using (2) and (1) yields:

$$\varphi = \left(\boldsymbol{\sigma} - \frac{\partial \Psi}{\partial \boldsymbol{\varepsilon}}\right) : \dot{\boldsymbol{\varepsilon}} - \left(S + \frac{\partial \Psi}{\partial T}\right)\dot{T} - \frac{\partial \Psi}{\partial \boldsymbol{\varepsilon}^p} : \dot{\boldsymbol{\varepsilon}}^p - \frac{\partial \Psi}{\partial \chi}\dot{\chi} - \frac{\partial \Psi}{\partial m}\dot{m} \geqslant 0 \tag{3}$$

In the case of a chemically inert material ($\dot{m} = 0$), and when no plastic evolutions occur, ($\dot{\boldsymbol{\varepsilon}}^p = 0, \dot{\chi} = 0$), the dissipation is zero ($\varphi = 0$), which leads to the standard state equations:

$$\boldsymbol{\sigma} = \frac{\partial \psi}{\partial \boldsymbol{\varepsilon}}; \quad S = -\frac{\partial \psi}{\partial T} \tag{4}$$

Equation (4) still hold in the case of a reactive porous material and when plastic evolutions occur, and (3) then reads:

$$\varphi = \boldsymbol{\sigma} : \dot{\boldsymbol{\varepsilon}}^p + \zeta\dot{\chi} + A_m\dot{m} \geqslant 0 \tag{5}$$

with:

$$\boldsymbol{\sigma} = -\frac{\partial \psi}{\partial \boldsymbol{\varepsilon}^p}; \quad \zeta = -\frac{\partial U}{\partial \chi}; \quad A_m = -\frac{\partial(\psi + U)}{\partial m} \tag{6}$$

where A_m = affinity of the chemical reaction which expresses in the macroscopic modeling the imbalance between the free water and the water combined in solid phase: it is the driving force of the considered micro-diffusion process of the hydration reaction. Furthermore, for a chemical inert material, (5) reduces to the dissipation of an ordinary solid with irreversible skeleton evolutions (see for instance Lemaitre and Chaboche, 1990), and the thermodynamic force ζ is called hardening force, which account for the evolution of the plastic threshold within the plastic criterion $f = f(\boldsymbol{\sigma}, \zeta) \leqslant 0$. In return and in contrast to standard hardening/softening plasticity, where the plastic threshold depends only on the plastic evolutions [i.e., $\zeta = \zeta(\chi)$], the material threshold may as well evolve due to the extent of the chemical reaction. This coupling between plastic evolutions and chemical reaction is called chemical hardening (Coussy and Ulm, 1996), and is expressed by a dependence of hardening force ζ on both plastic variable χ and hydrate mass m, i.e. $\zeta = \zeta(\chi, m)$. This leads to account for strength growth as chemo-plastic hardening in early-age concrete (Ulm and Coussy, 1996). In the same manner, other chemo-mechanical cross-effects can be considered, such as the strain induced by the hydration reaction (autogenous shrinkage), or the evolution of the elastic properties of the material (aging elasticity), as well as thermo-chemical couplings associated with the exothermal nature of the hydration reaction. From the standpoint of constitutive modeling, these couplings terms result from Maxwell-symmetries on free energy $\Psi = \psi + U$, since:

$$\frac{\partial \boldsymbol{\sigma}}{\partial m} = -\frac{\partial A_m}{\partial \boldsymbol{\varepsilon}} = \frac{\partial^2 \psi}{\partial \boldsymbol{\varepsilon}\,\partial m}; \quad \frac{\partial S}{\partial m} = \frac{\partial A_m}{\partial T} = -\frac{\partial^2 \psi}{\partial T\,\partial m}; \quad \frac{\partial \zeta}{\partial m} = \frac{\partial A_m}{\partial \chi} = -\frac{\partial^2 U}{\partial \chi\,\partial m} \tag{7}$$

which express the chemo-mechanical, chemo-thermal and chemo-plastic couplings. They will be detailed in the sequel.

2.1. *Chemo-elastic cross-effect*

The creation of hydration products leads to stiffening of the matter, which—at the macro-level of material description—appears as a variation of the elasticity modulus in time. At a micro-level of material description, this aging elasticity cannot be regarded as an actual change of the elastic material properties of the matter constituting concrete, but rather as a change in the concentration of the non-aging constituents (e.g. Bažant, 1995), i.e. the hardened cement gel. Furthermore, this change in concentration of the hardened cement gel is accompanied by a volume reduction (Le Chatelier contraction), coupled with a capillary shrinkage related to the formation of menisci due to water consumption through

hydration (e.g. Wittmann, 1982; Acker, 1988; Hua, 1992; Sicard *et al.*, 1996). Both aging elasticity and shrinkage related to the hydration reaction are chemo-mechanical cross-effects, expressed by the first of Maxwell-symmetry relations (7), which together with $(6)_1$, yields state equation $(4)_1$ in an incremental form:

$$\mathrm{d}\boldsymbol{\sigma} = \boldsymbol{C}:(\mathrm{d}\boldsymbol{\varepsilon} - \mathrm{d}\boldsymbol{\varepsilon}^p - \boldsymbol{a}\,\mathrm{d}T - \boldsymbol{b}\,\mathrm{d}m) \tag{8}$$

where $\boldsymbol{C} = \partial^2\psi/\partial\boldsymbol{\varepsilon}^2$ = elastic stiffness tensor (tangent with respect to strain $\boldsymbol{\varepsilon}$), which depends on the hydrate mass m, i.e., $\boldsymbol{C} = \boldsymbol{C}(m)$, as suggested from experiment (cf Byfors, 1980; Laube, 1990; Torrenti, 1992; Boumiz *et al.* 1996). Furthermore, the second order tensors $\boldsymbol{a}$ and $\boldsymbol{b}$ account for thermo-mechanical and chemo-mechanical cross-effects. In particular, $\boldsymbol{a} = -\boldsymbol{C}^{-1}:\partial^2\psi/\partial\boldsymbol{\varepsilon}\,\partial T$ is the tensor of (tangent) thermal dilatation coefficients, which relates the temperature variation $\mathrm{d}T$ to the macroscopic unrestrained strain of the thermal origin. In the same manner $\boldsymbol{b} = -\boldsymbol{C}^{-1}:\partial^2\psi/\partial\boldsymbol{\varepsilon}\,\partial m$ is the tensor of chemical dilatation coefficient which relates the increase in solidification mass m to the strains of chemical origin. In the isotropic case, for which $\boldsymbol{a} = a\mathbf{1}$ and $\boldsymbol{b} = b\mathbf{1}$, (8) reads after inversion:

$$\mathrm{d}\boldsymbol{\varepsilon} = \frac{\mathrm{d}\boldsymbol{s}}{2G(m)} + \frac{\mathrm{d}\sigma\mathbf{1}}{K(m)} + \boldsymbol{\varepsilon}^p + a\,\mathrm{d}T\mathbf{1} + b\,\mathrm{d}m\mathbf{1} \tag{9}$$

where $\boldsymbol{s}$ = stress-deviator, and σ = volume stress ($\boldsymbol{\sigma} = \boldsymbol{s} + \sigma\mathbf{1}$). Furthermore, $G = G(m)$ and $K = K(m)$ are the (tangent) shear modulus and bulk modulus, respectively. Boumiz *et al.* (1996) determined this coupling experimentally by measuring the elastic properties by ultrasonic measurements (compressive and shear waves), and the hydration degree by isothermal calorimetric tests.

2.2. *Chemo-plastic cross-effects*

For the modeling of early-age concrete cracking, two phenomena need to be taken into account: on the one side the irreversible skeleton evolution (i.e., microcracking) on the other side the evolution of the crack-threshold with the hydration extent. The first is taken into account here within the standard continuum approach of elastoplasticity, the second by chemo-plastic hardening/softening. More precisely, the chemo-plastic cross-effects concern the initial material threshold at the onset of plastic evolutions for a given hydration state, i.e. the strength growth strictly speaking, as well as the plastic hardening/softening properties of the material when irreversible skeleton evolutions occur. These couplings imply a dependence of the hardening force ζ on both plastic hardening/softening variable χ and hydrate mass m:

$$\zeta = -\frac{\partial U(\chi, m)}{\partial\chi} = \zeta(\chi, m) \tag{10}$$

Concerning the evolution of material strength, it has been shown that the compressive strength of concrete increases quasi-linearly with the hydration products (e.g., Mindess *et al.*, 1978), and thus, with hydrate mass m. Less has been reported on the evolution of the hardening/softening behavior of hydrating concrete. In a first approach, a linear chemo-plastic coupling can be assumed, such that:

$$\zeta = m\zeta_\infty - m\frac{\partial U_\infty(\chi)}{\partial\chi} \tag{11}$$

where $m\zeta_\infty$ = the strength growth as pure chemical hardening, and $-m\,\partial U_\infty(\chi)/\partial\chi$ its evolution due to plastic evolutions, both defined with respect to their values at complete hydration.

As in the standard plastic model, the plastic admissible stress states are defined by a loading function $f = f(\boldsymbol{\sigma}, \zeta) \leqslant 0$, and only plastic evolutions occur, if a loading point $\boldsymbol{\sigma}$ is at

the boundary of the elasticity domain and where it remains ($f = \mathrm{d}f = 0$). Therefore, standard expressions can be applied for both the flow rule and the hardening rule:

$$\mathrm{d}\boldsymbol{\varepsilon}^p = \mathrm{d}\lambda \frac{\partial g(\boldsymbol{\sigma}, \zeta)}{\partial \boldsymbol{\sigma}}; \quad \mathrm{d}\chi = \mathrm{d}\lambda \frac{\partial h(\boldsymbol{\sigma}, \zeta)}{\partial \zeta} \tag{12}$$

where $g(\boldsymbol{\sigma}, \zeta)$ and $h(\boldsymbol{\sigma}, \zeta)$ are the plastic and the hardening potential, respectively. In return, the plastic multiplier $\mathrm{d}\lambda$ and the hardening modulus H read in a modified form. In fact, the constituency condition $\mathrm{d}f = 0$ is written in the form (Coussy and Ulm, 1996):

$$\frac{\partial f}{\partial \zeta} \frac{\partial \zeta(\chi, m)}{\partial \chi} - \mathrm{d}_\chi = -\mathrm{d}_\chi f = -\mathrm{d}\lambda H \tag{13}$$

where $\mathrm{d}_\chi f$ = subdifferential of loading function f at constant values of hardening variable χ. Then using (11) and (12) in (13), yields:

$$\mathrm{d}\lambda = \frac{\mathrm{d}_\chi f}{H} = \frac{1}{H}\left[\frac{\partial f}{\partial \boldsymbol{\sigma}} : \mathrm{d}\boldsymbol{\sigma} + \frac{\partial f}{\partial \zeta} \zeta \frac{\mathrm{d}m}{m}\right] \tag{14}$$

$$H = mH_\infty \quad H_\infty = \frac{\partial f}{\partial \zeta}\left[\frac{\partial^2 U_\infty(\chi)}{\partial \chi^2}\right]\frac{\partial h}{\partial \zeta} \tag{15}$$

The first term in brackets on the right hand side of (14) corresponds to the standard format of the plastic multiplier in the plastic hardening/softening model, while the second term is due to chemo-plastic couplings. Note that the chemo-plastic model can be used without any further restrictions concerning loading function $f(\boldsymbol{\sigma}, \zeta)$, plastic potential $g(\boldsymbol{\sigma}, \zeta)$ and hardening potential $h(\boldsymbol{\sigma}, \zeta)$ than those imposed for the standard plastic model, i.e., convexity and non-negativity of the intrinsic dissipation associated with the plastic evolutions. The latter reads for $f = \mathrm{d}f = 0$:

$$\varphi_1 \, \mathrm{d}t = \boldsymbol{\sigma} : \mathrm{d}\boldsymbol{\varepsilon}^p + \zeta \, \mathrm{d}\chi = \mathrm{d}\lambda \left(\boldsymbol{\sigma} : \frac{\partial g}{\partial \boldsymbol{\sigma}} + \zeta \frac{\partial h}{\partial \zeta}\right) \geqslant 0 \tag{16}$$

which, owing to the non-negativity of plastic multiplier $\mathrm{d}\lambda$, defines the thermodynamic admissible directions $\partial g/\partial \boldsymbol{\sigma}$ and $\partial h/\partial \zeta$ of the plastic increments $\mathrm{d}\boldsymbol{\varepsilon}^p$ and $\mathrm{d}\chi$, according to the flow and hardening rule (12).

2.3. *Thermo-chemical cross-effects*

The entropy balance equation of the closed porous medium around a reference temperature T_0 reads:

$$T_0 \frac{\mathrm{d}S}{\mathrm{d}t} = Q^0 + \varphi \tag{17}$$

where $\mathrm{d}S$ = the internal entropy variation, $Q^0/T_0 = (r - \operatorname{div} \boldsymbol{q})/T_0$ = the rate of external entropy supply provided by heat exchange with the exterior, in form of volumic heat sources (for instance, cooling pipes, rate r) and by heat condition (heat flux $\boldsymbol{q} = -K \operatorname{grad} T$; K = conductivity), while φ/T_0 = the rate of internal entropy production due to dissipation φ [i.e. (5)]. Using (4) and (7) yields:

$$C_\varepsilon \dot{T} - T_0 \boldsymbol{A} : (\dot{\boldsymbol{\varepsilon}} - \dot{\boldsymbol{\varepsilon}}^p) - L_m \dot{m} = Q^0 + \varphi \tag{18}$$

The physical significance of the terms on the left-hand side of (18) have been detailed in Ulm and Coussy (1995), in particular:

- $C_\varepsilon = -T_0\, \partial^2\psi/\partial T^2$ = volume heat capacity per unit of volume (i.e., the heat required for a unit temperature variation);
- $T_0 \boldsymbol{A} = T_0\, \partial^2\psi/\partial T\, \partial\boldsymbol{\varepsilon}$ = the latent heat per unit of (elastic) deformation $\mathrm{d}\boldsymbol{\varepsilon} - \mathrm{d}\boldsymbol{\varepsilon}^p$, which constitutes the counterpart of the thermo-mechanical coupling with $\boldsymbol{A} = -\mathbf{C} : \mathbf{a}$ the stress per unit of temperature variation $\mathrm{d}T$ induced be restrained thermal dilatation. However, with respect to the small order of magnitude of elastic strains in cementious materials ($\|\boldsymbol{\varepsilon} - \boldsymbol{\varepsilon}^p\| < 0.001$) this coupling can be considered as negligible as far as the heat equation is concerned;
- $L_m = T_0\, \partial^2\psi/\partial T\, \partial m$ = the latent heat of the hydration reaction per unit of solidification mass $\mathrm{d}m$, which accounts for the exothermic nature ($L_m > 0$) of the hydration reaction in the macroscopic modeling, in addition to the heat associated with the hydration dissipation (i.e., $A_m \dot{m} \geqslant 0$), even though the latter can be considered as negligible with respect to the former exothermic latent hydration heat (i.e. $|A_m| \ll L_m$). The same reasoning can be applied to the dissipation associated with the irreversible skeleton evolution, φ_1 [i.e., (16)], as well as to the latent heat of (elastic) deformation, which both can be considered as negligible with respect to the latent hydration heat. In this case, heat eqn (18) simplifies to:

$$C_\varepsilon \dot{T} = Q^0 + L_m \dot{m} \tag{19}$$

which—as we will see hereafter—lends itself readily for the experimental determination of thermo-chemical couplings.

3. IDENTIFICATION OF THE MACROSCOPIC HYDRATION KINETICS

As stated before, the hydration reaction governs the evolution of the mechanical properties of concrete; it leads to shrinkage, and generates heat due to the exothermic nature of the reaction. The prediction of the hydration evolution (i.e., hydration kinetics) is therefore a matter of main concern.

3.1. *Hydration kinetics. Hydration degree*

The hydration reaction may be roughly viewed as follows: at instant t, the solid part of the matter is formed of unhydrated cement and hydrates. In order for the reaction to occur, water (as well as dissoluted ions) diffuses through the layers of hydrates already formed to the unhydrated cement. Once they meet, new hydrates are formed according to a thermally activated reaction; then the water is chemically and/or physically combined. Hence, the diffusion of water through the layers of hydrates can be considered as the rate-determining process of the hydration kinetics. Thermodynamic considerations of chemically reactive porous media (Coussy, 1995) lead to the postulate that the hydration of concrete, under sealed conditions, is governed by two constitutive laws. On the one side the law that describes the kinetics. It links the rate $\dot{m}$ of the current hydrate mass m to the affinity A_m of the reaction. Applied to early-age concrete, A_m can be roughly viewed as the difference between the chemical potentials of the free water and the water combined in the solid phase, and is the driving force of the micro-diffusion process. The kinetics law is assumed to be of the form (Ulm and Coussy, 1995):

$$A_m = \eta(m) \frac{\mathrm{d}m}{\mathrm{d}t} \exp\left(\frac{E_a}{RT}\right) \tag{20}$$

where E_a = the activation energy, and R = ideal gas constant. The factor $\exp(E_a/RT)$

accounts for the thermically activated character of the reaction according to the Arrhenius concept, while the factor $\eta(m)$, an increasing function of m, accounts for the increase of the thickness of the hydrate layers already formed, which increases the (micro-)diffusion time of the free water to reach the unhydrated cement.

The second constitutive law is the state equation which relates the hydration affinity A_m to the current hydrate mass m. Due to the different cross-effects detailed above as a consequence of the Maxwell-symmetries in (7), affinity A_m may as well depend on the elastic strain $\boldsymbol{\varepsilon}-\boldsymbol{\varepsilon}^p$ (respectively, on stress $\boldsymbol{\sigma}$), on the temperature variation $T-T_0$ and on the hardening variable χ. As a first approximation, the affinity is assumed to depend significantly only on hydrate mass m, while the effect of (sustained) stress, temperature variation and plastic hardening/softening (i.e., microcracking) may be assumed to be negligible (for a discussion of this weak coupling hypothesis, see Ulm and Coussy, 1995), thus:

$$A_m \cong A_0 - a(m) \tag{21}$$

The affinity A_m as the driving force of the reaction decreases progressively from its initial value, A_0, which in turn depends on the concrete composition. Furthermore, the reaction stops when the affinity takes zero values, which corresponds to thermodynamic equilibrium. Denoting m_∞ the asymptotic hydrate mass, it follows:

$$A_0 = a(m_\infty) \tag{22}$$

Due to the assumed independence of affinity A_m on other variables than hydrate mass m, the asymptotic mass m_∞ is independent of the thermal and loading history of the material. It is the same for two identical concrete samples (hydrically insulated), provided the same initial affinity A_0 (i.e. roughly, concrete samples from the same batch). Therefore, for a given composition, the hydration degree can be intrinsically defined by:

$$\xi = \frac{m}{m_\infty} \quad 0 \leqslant \xi \leqslant 1 \tag{23}$$

Hence, as the weight fraction of hydrate mass m with respect to its asymptotic value, as defined in cement chemistry (Powers and Brownyard, 1948), with $m_\infty \cong 0.25 m_c$; m_c = initial cement mass per unit of volume). Definition (23) provides therefore the link between the experimental observation on thermo-chemical-mechanical cross-effects and the constitutive modeling. Furthermore, it allows one to rewrite the kinetics law (20) in the form:

$$\tilde{A}(\xi) = \dot{\xi} \exp\left(\frac{E_a}{RT}\right) \tag{24}$$

where $\tilde{A}(\xi)$ can be considered as normalized affinity, which account for the driving force of the microdiffusion process [i.e., (21)], as well as for the increase of the diffusion time [i.e. $\eta(m)$]. Finally, it may be useful to introduce the so-called maturity μ (in fact a sort of normalized time), widely used to describe the effects of the hydration kinetics on the evolution of the mechanical properties of concrete. It is defined by:

$$\mu = \int_0^t \exp\left[\frac{E_a}{R}\left(\frac{1}{T_0} - \frac{1}{T(\tau)}\right)\right] d\tau \tag{25}$$

where T_0 is a reference temperature for which μ coincides with time t. Using (25) in (24) reduces the kinetics law to an ordinary differential equation:

$$\frac{d\xi}{d\mu} = c\tilde{A}(\xi) \tag{26}$$

where $c = \exp(-E_a/RT_0) = \text{const}$, and reveals the existence of an unique relation between the maturity μ and hydration degree ξ:

$$\xi = \xi(\mu) \tag{27}$$

Thus, two samples made of the same concrete which have the same maturity, have undergone equivalent thermal histories (i.e., curing) with respect to the hydration process: their hydration degree is the same.

3.2. *Experimental determination of the hydration kinetics*

The prediction of the hydration degree, and thus its effects on strain, strength growth and heat generation, requires the knowledge of the function $\tilde{A}(\xi)$, which is assumed to be an intrinsic kinetics function (i.e., independent of particular field and associated boundary conditions). However, on the macroscopic scale of a concrete sample, the hydration kinetics can be followed only indirectly through the effects the phenomenon induces, i.e. through its cross-effects with heat generation, strength evolution or autogenous shrinkage. In terms of the theory presented here, the kinetics function $\tilde{A}(\xi)$ can be determined by exploring the Maxwell-symmetries of the modeling, provided that the order of the coupling is known (Ulm and Coussy, 1996). This is illustrated here for adiabatic calorimetric experiments and isothermal strength growth evolution tests. The test-data used hereafter are taken from Laplante (1993).

3.2.1. *Adiabatic calorimetric experiment* The determination of the hydration degree from alorimetric tests is the current standard, and consists in exploring the linear thermochemical couplings in heat eqn (19), which on account of the variable change $m \to \xi$ becomes

$$C_v\dot{T} = Q^0 + L\dot{\xi} \tag{28}$$

where $L = L_m m_\infty$ = the latent heat per unit of hydration degree $d\xi$, while Q^0 = the rate of external heat supply. In an adiabatic experiment, in which $Q^0 = 0$, the exothermal nature of the hydration reaction ($L > 0$), leads to a temperature rise, as illustrated in Fig. 1, for

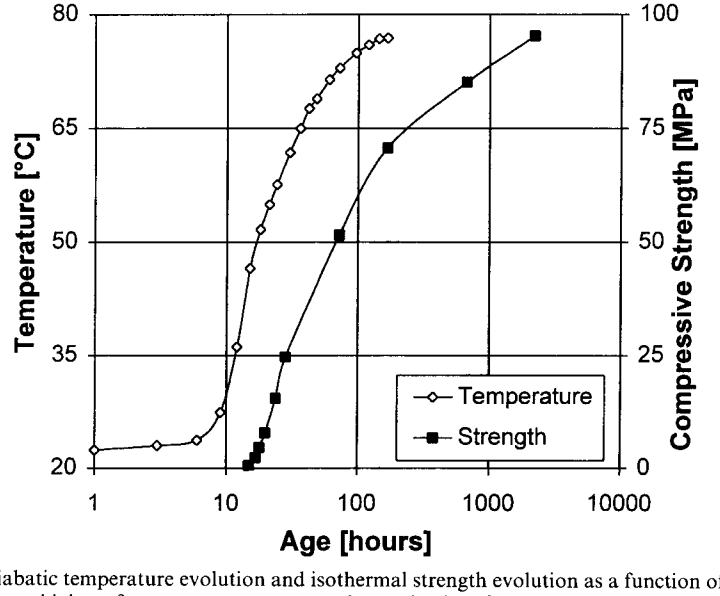

Fig. 1. Adiabatic temperature evolution and isothermal strength evolution as a function of time for a high performance concrete (experimental values from Laplante, 1993).

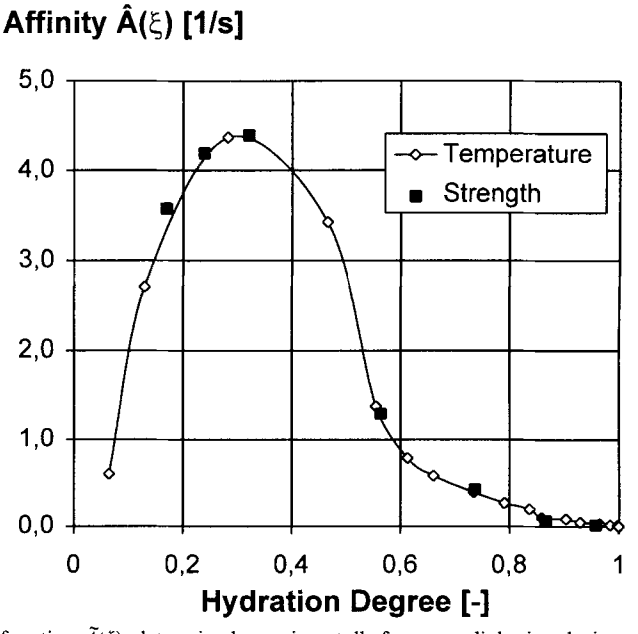

Fig. 2. Kinetic function $\tilde{A}(\xi)$, determined experimentally from an adiabatic calorimetric experiment ("temperature"), and from the isothermal strength evolution ("strength").

a high performance concrete (water/cement ratio = 0.3, silica fume/cement ratio = 0.1). Assuming the volume heat capacity C_ε and the latent hydration heat $L = C_\varepsilon(T_\infty - T_0)$ are constant, (28) leads to:

$$\xi(t) = \frac{T^{ad}(t) - T_0}{T_\infty - T_0} \tag{29}$$

where $T^{ad}(t)$ = the temperature measured in such an experiment, while T_0 and T_∞ are, respectively, the initial temperature and the asymptotic temperature in the considered adiabatic experiment. In addition, using (29) in (24) yields:

$$\tilde{A}(t) = \frac{\mathrm{d}T^{ad}(t)/\mathrm{d}t}{T_\infty - T_0} \exp\left(\frac{E_a}{RT^{ad}(t)}\right) \tag{30}$$

With $T^{ad}(t)$ being a measured function of time, eqns (29) and (30) provide a direct experimental access to the kinetics function $\tilde{A}(\xi)$ in a parameter form of time t of the adiabatic experiment. This is shown in Fig. 2 (curve labeled "temperature"). The activation energy E_a utilized for the determination corresponds to $E_a/R = 4000$ K, and is the average apparent activation energy, determined previously for this kind of concrete (Laplante, 1993).

3.2.2. *Isothermal strength evolution* The previous determination assumes the validity of the approach. In fact, another experiment, independent of the former, is required, in order to confirm the intrinsic character of the found kinetics function $\tilde{A}(\xi)$. To this end, we consider the isothermal strength evolution of the same concrete, as shown in Fig. 1 (curve labeled "strength"). More precisely, experiments have shown that the compressive strength f_c evolves according to (Regourd and Gauthier, 1980):

$$\frac{\mathrm{d}f_c}{\mathrm{d}t} = F(f_c) \exp\left(-\frac{E_a}{RT_0}\right) \tag{31}$$

where T_0 is the temperature at which the experiments were performed. This experimental

observation states that the kinetics of strength evolution is related to the hydration kinetics [i.e., (20)], provided that the compressive strength depends unequivocally on hydrate mass m. In fact, this relation has been established experimentally from isothermal strength evolution tests. In particular, beyond a solidification threshold (also called percolation threshold, cf Acker, 1988), the increase in compressive strength df_c during time dt is found to be proportional to the increase in hydration products, i.e. dm, or equivalently [see (23)] to the increase in hydration degree $d\xi$:

$$\frac{df_c}{dt} = \rho \frac{d\xi}{dt} \tag{32}$$

where $\rho(>0)$ is a constant. In the theory, (31) and (32) are taken into account by the linear dependence of hardening force ξ on hydration mass m [i.e., (11)], the evolution of which is given by kinetics law (20). Exploring this linear chemo-plastic coupling for the material strength $\zeta = m(f_{c\infty} - f_{c0})$, relation (32) together with (23) and (11) yield a second access to hydration degree $\xi(t)$ from the isothermal compressive strength evolution $f_c(t)$:

$$\xi(t) = \frac{\zeta(t)}{\zeta_\infty} = \frac{f_c(t) - f_{c0}}{f_{c\infty} - f_{c0}} \tag{33}$$

with $f_{c\infty}$ the compressive strength at complete hydration. Furthermore, $f_{c0}(\leqslant 0)$ is a reference value for $\xi = 0$, which accounts for the experimentally observed percolation threshold ξ_0 of the matter ($\xi_0 = -f_{c0}/\rho$). Equation (33) is of the same format as eqn (29), and provides a second independent access to kinetics function $\tilde{A}(\xi)$ in a parameter form of time t of the isothermal experiment:

$$\tilde{A}(t) = \frac{df_c(t)/dt}{f_{c\infty} - f_{c0}} \exp\left(\frac{E_a}{RT_0}\right) \tag{34}$$

This is shown in Fig. 2 (curve labeled "strength"). The values for $\tilde{A}(\xi)$ determined for this concrete from two independent experiments, a calorimetric and a mechanical one, coincide and confirm the intrinsic nature of the kinetics function $\tilde{A}(\xi)$. This agreement must be seen in perspective with the time scale of the observation of the adiabatic calorimetric experiment and the isothermal strength evolution tests (see Fig. 1): due to the thermal activation of the hydration reaction, the hydration rate is much higher under adiabatic conditions than under isothermal conditions. The obtained result thus confirms the insignificant influence of temperature T on affinity A_m and thus, the validity of the weak coupling hypothesis on temperature T used to derive (23) and (24).

The previous determination of the hydration kinetics can be extended to other couplings between the hydration reaction and macroscopic observable (i.e. accessible) phenomena provided that the order of coupling is known. And vice versa: the intrinsic nature of kinetics function $\tilde{A}(\xi)$ gives access to the hydration degree irrespective of any particular boundary condition, and allows for the determination of other chemo-mechanical couplings, as the coupling at the origin of the autogenous shrinkage or that related to the elastic properties. These couplings are shown in Fig. 3, for the concrete considered before, with the hydration degree being determined from the isothermal compressive strength evolution [i.e. eqn (33)]. The slope of the autogenous shrinkage curve presents with opposite sign the chemical dilatation coefficient $\beta = bm_\infty$, with b defined by state eqn (9).

4. THERMO-CHEMO-MECHANICAL COUPLINGS IN STRUCTURAL DESIGN

So far, thermo-chemo-mechanical couplings have been treated from the standpoint of macroscopic constitutive modeling of temperature, deformation and cracking in early age concrete. The proposed approach allowed for the experimental *in vitro* identification of affinity $\tilde{A}(\xi)$ as an intrinsic material function that describes the macroscopic hydration

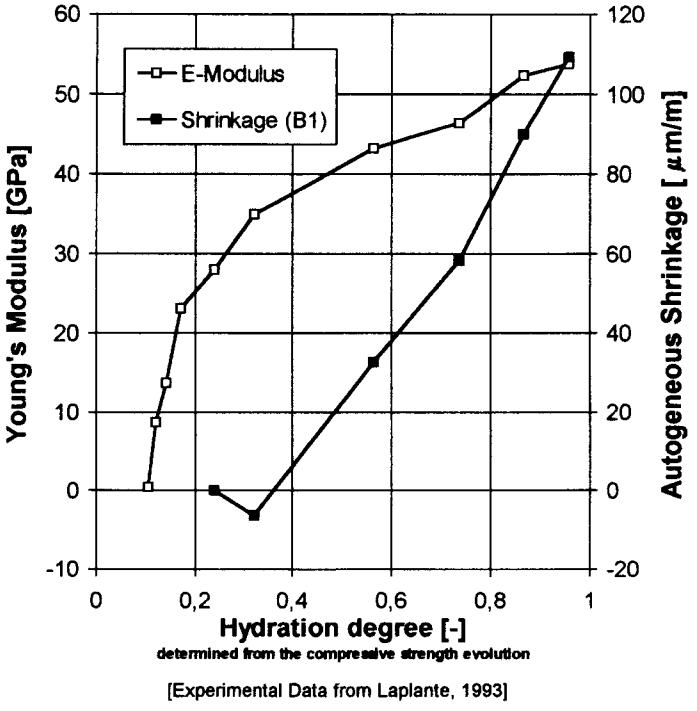

Fig. 3. Chemo-mechanical cross-effects: Young's modulus and autogenous shrinkage as a function of the hydration degree (experimental values from Laplante, 1993).

kinetics. Owing to its intrinsic nature, the function can be used for the *in situ* prediction of the hydration degree under other field conditions than those applied to the laboratory test specimens, and to account for thermo-chemo-mechanical cross-effects in the design of early-age concrete structures. In fact, the optimization of the performance of concrete structures at early ages involves both the optimization of the material for a given structure, boundary conditions and structural constraints, and—vice versa—the optimization of the structure for a given material behavior. For the first, the material behavior needs to be broken down to its intrinsic components, such as kinetics function $\tilde{A}(\xi)$, which can be used to compare the hydration kinetics of different concrete-mixes, and thus the evolution rate of the mechanical properties under field conditions prevailing in a structure. The optimization of the structural performance requires numerical analysis and reliable design criteria for early-age concrete structures. The latter may be derived considering the thermo-chemo-mechanical couplings on the scale of engineering structures.

For the numerical application, in a first approach use can be made of the weak coupling hypothesis (19) and (21), and allows one to solve the thermo-chemical problem independent of the mechanical one. The coupled thermo-chemical problem consists in solving simultaneously field eqn (19) and (local) kinetics law (24), and leads to the numerical determination of the temperature field and the hydration degree. Here, standard numerical procedures can be applied: a discretization in space by the finite element method with standard boundary conditions concerning temperature and heat flux through the boundary (i.e., casting moulds); and a Crank–Nicholson integration scheme in time for both temperature and hydration degree evolution. These results are used in the mechanical problem to generate stresses of thermal and chemical origin, on account of the elastic stiffening of the material as a function of the hydration degree; and standard return mapping schemes (Ortiz and Simo, 1986) together with consistent tangent operator (Simo and Taylor, 1985) can be readily adapted for the integration of the chemo-plastic constitutive equations (Meschke, 1996; Hellmich *et al.* 1997).

The example presented hereafter is part of a research program conducted at LCPC on behalf of the French national railroad company, S.N.C.F. (Ulm *et al.*, 1996). It concerns the structural optimization of tunnel-platforms in steel-fiber reinforced high performance

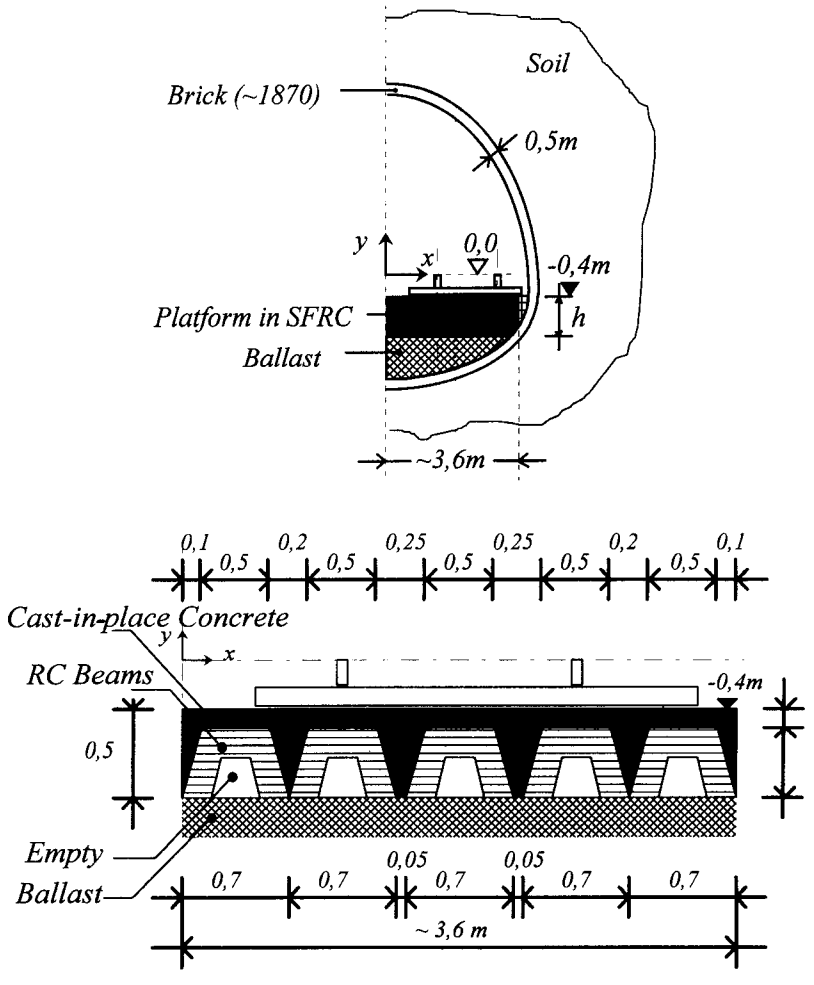

Fig. 4. Case studies of a railroad tunnel-platform: (a) plain concrete solution; (b) U-profiled precast RC-beams covered by cast-in-place concrete.

concrete (SFR-HPC). Several configurations were studied, among which are the two illustrated in Fig. 4(a) and (b): the solution shown in Fig. 4(a) consists of a plain concrete platform cast in place on existing ballast. The structure shown in Fig. 4(b) consists of reversed U-profiled precast RC-beams, empty to the inside and covered by cast-in-place concrete to the outside.

Finite element analyses have been performed in order to determine the temperature field, the hydration degree and the induced mechanical effects. Figure 5(a) shows the results obtained from the thermo-chemical analysis, in terms of temperature $T(t) - T_0$ vs hydration degree $\xi(t)$ for the highest local temperature rise in the structure, both being direct results of the analysis. Note, that the bisecting line ($x = y$) corresponds to adiabatic boundary conditions [i.e. $Q^0 = 0$ in eqn (19)], while the x-axis corresponds to isothermal evolutions [i.e. $\dot{T} = 0$ in eqn (19)]. The results show a quasi-adiabatic behavior of the plain concrete solution up to high hydration degrees, while the U-profiled precast solution leads to lower temperature rises, and a cooling that starts at lower hydration degrees. This is due to the structural capacity to evacuate heat, as illustrated in Fig. 5(b), that shows the heat evacuated by conduction as a function of the hydration degree, obtained for the local temperature evolutions shown in Fig. 5(a). Note that the bisecting line here corresponds to the ideal case of isothermal conditions, while the x-axis corresponds to adiabatic boundary conditions. Hence, from these analyses of thermo-chemical couplings, the U-profiled precast solution can be considered as optimized in terms of its structural heat evacuation capacity.

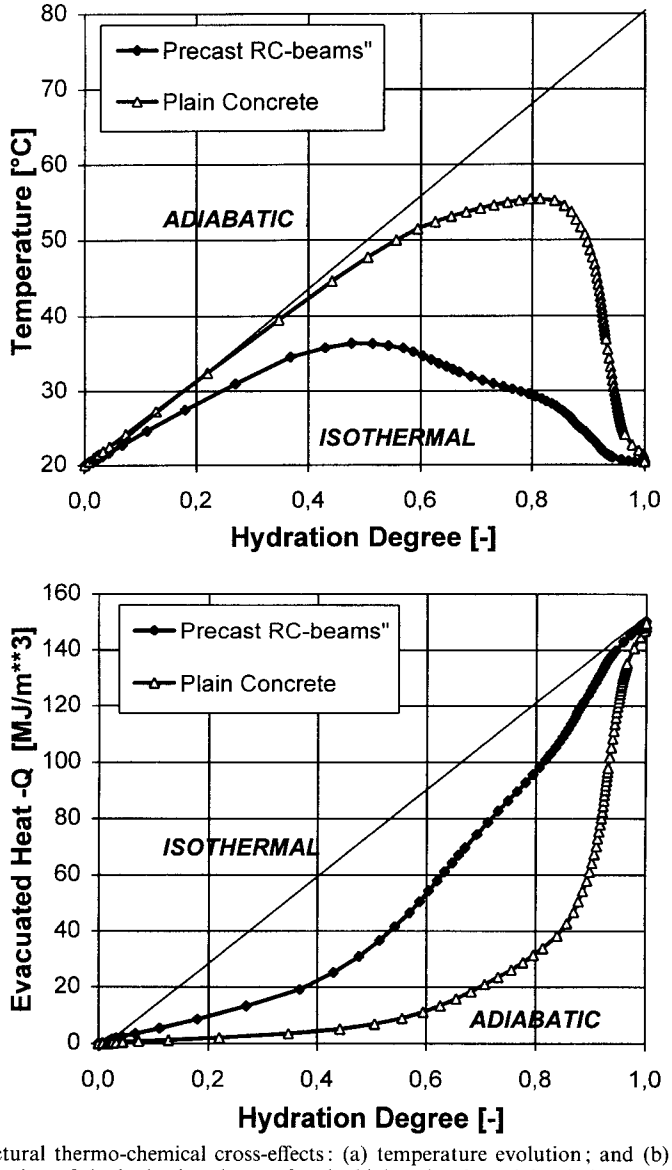

Fig. 5. Structural thermo-chemical cross-effects: (a) temperature evolution; and (b) conduction heat as a function of the hydration degree, for the highest local (nodal point) temperature rise in the structure.

This capacity related to the structural dimension is straightforwardly quantified by dimensional analysis applied to heat eqn (28). In fact, neglecting volume heat sources, the latter reads on account of the kinetics law (24) and when using the linear (Fourier) heat conduction law:

$$C_\varepsilon \frac{\mathrm{d}T}{\mathrm{d}t} = K\Delta_x T + L\tilde{A}(\xi)\exp\left(-\frac{E_a}{RT}\right) \tag{35}$$

where Δ_x = the Laplacian operator. Then using the dimensionless variables $\mathbf{X} = \boldsymbol{x}/\mathscr{L}$ and $\tau = t/\mathscr{T}$ for the space and the time derivative in (35) yields:

$$\frac{\partial T}{\partial \tau} = \Delta_X T + L\frac{\mathscr{T}}{C_\varepsilon}\tilde{A}(\xi)\exp\left(-\frac{E_a}{RT}\right) \tag{36}$$

where $\Delta_X = \Delta_x/\mathscr{L}^2$ = the Laplacian operator defined with respect to the dimensionless

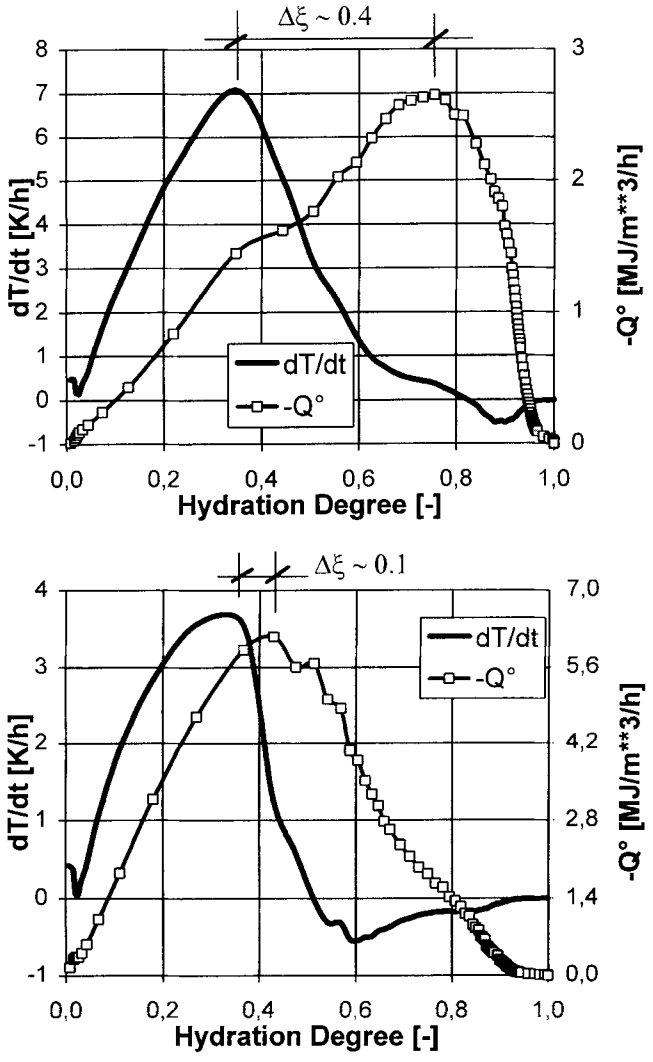

Fig. 6. Structural heat evacuation capacity: temperature rate and heat conduction rate as a function of the hydration degree for (a) the plain concrete solution and (b) the precast RC-beam solution (same nodal points as for Fig. 5).

space variable **X**, while $\mathscr{T}$ and $\mathscr{L}$ are, respectively, the characteristic time and the characteristic length of heat conduction, related in a standard manner by:

$$\mathscr{T} = \frac{\mathscr{L}^2}{K/C_\varepsilon} \tag{37}$$

Equation (36) shows that the latent hydration heat effects (i.e. the thermo-chemical cross-effects) increase linearly with the characteristic conduction time $\mathscr{T}$, and thus, quadratically with the structural dimension, $\mathscr{L}$. This is illustrated in Fig. 6(a) and (b), which show the temperature rate $\dot{T}$ and the heat rate $-Q^0$ (negative heat supply rate) transported by conduction to the exterior as a function of the hydration degree, for the plain concrete solution (Fig. 6(a)) and the U-profiled precast solution (Fig. 6(b)) for the highest local temperature rise in both structures. The peak of the temperature rate curve corresponds roughly to the highest hydration heat production [i.e., $\mathrm{d}\tilde{A}(\xi)/\mathrm{d}\xi = 0$], while the peak of the heat rate curve is related to the solidification state at which the heat evacuation by conduction becomes superior to the internal hydration heat production. In the ideal case in which these peaks coincide, any hydration heat production is carried away to the outside by conduction (which corresponds to isothermal evolutions). Hence, the distance between

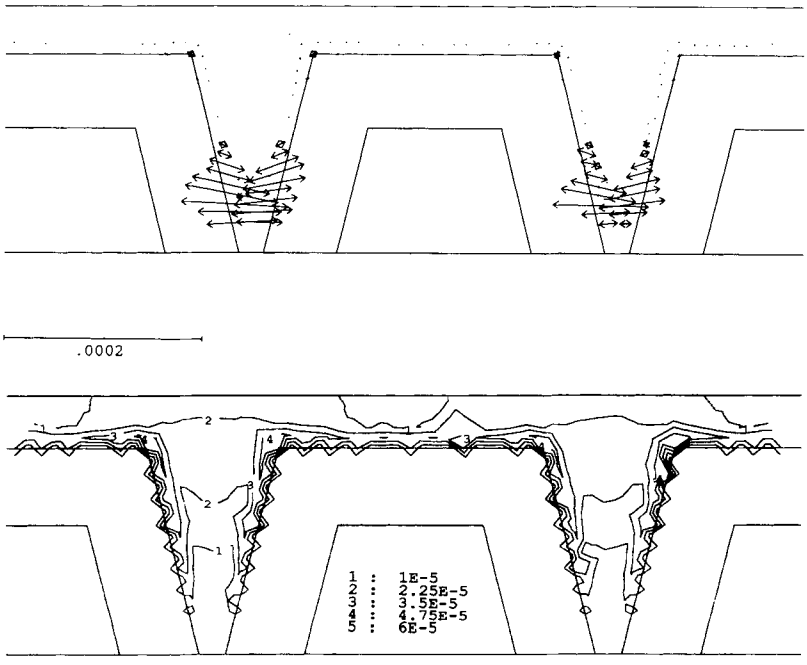

Fig. 7. Plastic strains modeling the concrete cracking at early ages: (a) the principal plastic strains at 24 h after casting; (b) isovalues of plastic strains in the z-direction (plane strain conditions) at 50 days after casting.

these peaks leads to temperature rises, which are only related to the dimension of the structure: it is the increase in hydration degree during the characteristic time of heat conduction $\mathcal{T}$, and can be optimised in structural design.

Finally, Fig. 7(a) and (b) show the plastic strains obtained from the thermo-chemo-mechanical analysis for the optimised U-profiled precast solution. In this analysis the three parameter Willam–Warnke criterion (Willam and Warnke, 1975) with chemical hardening has been used for concrete. In particular, Fig. 7(a) shows the mechanical effect of restrained thermal swelling at 24 h after casting at the interface of the precast RC-beams and the cast-in-place concrete, in terms of the first principal plastic strain, normal to which cracking planes form. These cracks partly reclose during thermal shrinkage. Figure 7(b) shows the plastic strain in the z-direction at 50 days after casting, which results from the shrinkage under plane strain conditions (continuous casting). However, due to the low hydration degree at which cooling starts (see Fig. 5(a)), these effects remain limited to narrow zones at the interface of the U-profiled precast beams and the concrete.

5. CONCLUDING REMARKS

This paper explored thermo-chemo-mechanical cross-effects in early age concrete at different levels, from the level of macroscopic material modeling to the level of structural design. Concerning the material modeling, these cross-effects result from Maxwell-symmetries. They characterize the autogenous shrinkage, hydration heat and strength growth due to the chemo-mechanical, thermo-chemical and chemo-plastic couplings with a minimum of material parameters accessible by standard material tests. Moreover, provided that the order of coupling is known, the latter can be used to determine in an intrinsic manner the macroscopic hydration kinetics of concretes. This has been shown by considering adiabatic calorimetric experiments and isothermal strength growth tests, which lead to the determination of the same kinetics function. The proposed approach can be extended to other chemo-mechanical couplings in concretes, where a chemical reaction induces mechanical effects (for instance the alkali–aggregate reaction or leaching phenomena). Finally, these cross-effects can be followed up to the structural level, and allows one

to optimize the design of concrete structures at early ages. In particular, exploring the thermo-chemical cross-effects at this structural level can quantify the conduction heat capacity of structures with respect to hydration heat effects, which may be used as a design criterion to minimize early age concrete cracking. Finally, creep effects were not yet considered in the modeling. They can be found in Bažant *et al.* (1996), extending the standard solidification theory of concrete creep (Bažant and Prasannan, 1989 a, b) to aging viscous flow due to micro-prestress relaxation within the concrete matrix. Obviously, this prestressing of the matrix is related to the hydration reaction, and constitutes another chemo-mechanical cross-effect at the micro-level of material description—to be explored at the macrolevel of material modeling within the framework of reactive porous media.

Acknowledgements—This work was partly done in a joint research project of the Réseau des Laboratoires des Ponts et Chaussées (LPC) and the GEO research laboratory network. Furthermore, the design of the tunnel-platform is part of a feasibility study done at LCPC on behalf of the Société Nationale des Chemins de Fer (S.N.C.F.), France. Finally, the numerical analysis were achieved using the finite element program CESAR-LCPC. We are grateful to Dr Pierre Humbert of the Department for Numerical Models at LCPC for assisting the implementation of the chemoplastic model in CESAR-LCPC.

REFERENCES

Acker, P. (1988) Mechanical behavior of concrete : a physico-chemical approach. *Res. Rep. LPC* **152,** Laboratoires des Ponts et Chaussees, Paris, France.

Bažant, Z. P. (1995) Creep and damage in concrete. In *Material Science of Concrete IV*, ed. J. Skalney and S. Mindess, pp. 335–389. American Ceramic Society, Westerville, Ohio.

Bažant, Z. P. and Prasannan, S. (1989a) Solidification theory for concrete creep. I : Formulation. *Journal of Engineering Mechanics, ASCE* **115**(8), 1691–1703.

Bažant, Z. P. and Prasannan, S. (1989b) Solidification theory for concrete creep. II : Verification and application. *Journal of Engineering Mechanics, ASCE* **115**(8), 1704–1725.

Bažant, Z. P. Hauggaard, A. B., Baweja, S. and Ulm, F.-J. (1996) Microprestress—solidification theory for aging and drying effects on concrete creep. *Journal of Engineering Mechanics, ASCE*, in press.

Boumiz, A., Vernet, C. and Cohen Tenoudji, F. (1996) Mechanical properties of cement pastes and mortars at early ages. Evolution with time and degree and degree of hydration. *Advn. Cem. Bas. Mat.* **3,** 92–106.

Byfors, J. (1980) Plain concrete at early ages. Res. Rep., F3 : 80, Swedish Cement and Concrete Res. Inst., Stockholm, Sweden.

Coussy, O. (1995) *Mechanics of Porous Continua.* John Wiley and Sons, Chichester, U.K.

Coussy, O. and Ulm, F.-J. (1996) Creep and plasticity due to chemo-mechanical couplings. *Archive of Applied Mechanics* **66,** 523–535. Springer Verlag, Berlin.

Hellmich, Ch., Ulm, F.-J. and Mang, H. A. (1997) Chemoplasticity for shotcrete at early ages. *Computational Plasticity. Fundamentals and Applications* (Proc. 5th Int. Conf. on Comput. Plasticity, Barcelona, March 1997), ed. D. R. J. Owen, E. Onate, and E. Hinton, 1499–1507. CIMNE Barcelona.

Hua, C. (1995) Analysis and modeling of autodessiccation shrinkage of hardening cement paste. *Res. Rep. LPC*, OA15. Laboratoires des Ponts et Chaussees, Paris, France (in French).

Laplante, P. (1993) Mechanical properties of hardening concrete : a comparative analysis of ordinary and high performance concretes. *Res. Rep. LPC*, OA13. Laboratoires des Ponts et Chaussees, Paris, France (in French).

Laube, M. (1990) Constitutive model for the analysis of temperature-stresses in massive structures. Ph.D. thesis, Tu Braunschweig, Braunschweig, Germany (in German).

Lemaitre, J. and Chaboche, J. L. (1990) *Mechanics of Solid Materials.* Cambridge University Press, London, U.K.

Meschke, G. (1996) Consideration of aging of shotcrete in the context of a 3-D viscoplastic material model. *International Journal of Numerical Methods in Engineering* **39,** 3123–3143.

Mindess, S., Young, J. F. and Lawrence, F.-V (1978) Creep and drying shrinkage of calcium silicate pastes. I : Specimen preparation and mechanical properties. *Cement and Concrete Res.* **8,** 591–600.

Ortiz, M. and Simo, J. (1986) An analysis of a new class of integration algorithms for elastoplastic constitutive relations. *International Journal of Numerical Methods in Engineering* **23,** 353–366.

Powers, G. and Brownyard, T. L. (1948) Studies of the physical properties of hardened Portland cement paste. *Portland Cement Association*, Res. Bull. 22.

Regourd, M. and Gauthier, E. (1980) Behavior of cement under accelerated hardening. *Annales de l'ITBTP* **179,** 65–96, Paris, France (in French).

Sicard, V., Cubaynes, J. F., Pons, G. (1996) Modeling of delayed strains in high performance concrete : relation between shrinkage and creep. *Materials and Structures* **29**(7), 345–353 RILEM (in French).

Simo, J. and Taylor, R. (1985) Consistent tangent operator for rate independent elasto-plasticity. *Comp. Meth. in Appl. Mech. and Eng.* **48,** 101–118.

Torrenti, J.-M. (1992) Strength of concrete at very early ages. *Bulletin de Liaison des Laboratoires des Ponts et Chaussees* **179,** 31–41 Paris, France (in French).

Ulm, F.-J. and Coussy, O. (1995) Modeling of thermo-chemo-mechanical couplings of concrete at early ages. *Journal of Engineering Mechanics, ASCE* **121**(7), 785–794.

Ulm, F.-J. and Coussy, O. (1996) Strength growth as chemo-plastic hardening in early age concrete. *Journal of Engineering Mechanics, ASCE* **122**(12), 1123–1132.

Ulm, F.-J., Rossi, P. and Guerrier, F. (1996) Feasibility study of SNCF-tunnel platforms in steel-fiber-reinforced concrete. Res. Rep. LCPC/SNCF, Paris, France (in French).

Willam, K. J. and Warnke, E. P. (1975) Constitutive model for the triaxial behavior of concrete. *IABSE Proc.* 19, Paper III-1. Int. Ass. of Bridge and Struct. Eng., Sem. on Concr. Structures subject to triaxial stresses, Bergamo, Italy.

Wittmann, F. H. (1982) Creep and shrinkage mechanisms. In *Creep and Shrinkage of Concrete Structures*, ed. Z. P. Bažant and F. H. Wittmann, pp. 129–161. John Wiley and Sons.